Spin relaxation times of 2D holes from spin sensitive bleaching of inter-subband absorption

Petra Schneider[1], J. Kainz[1], S.D. Ganichev[1,2], V.V. Bel'kov[2],
S.N. Danilov[1], M.M. Glazov[2], L.E. Golub[2], U. Rössler[1],
W. Wegscheider[1], D. Weiss[1], D. Schuh[3], and W. Prettl[1]

[1] *Fakultät Physik, University of Regensburg, 93040 Regensburg, Germany*

[2] *A.F. Ioffe Physico-Technical Institute, 194021 St. Petersburg, Russia*

[3] *Walter Schottky Institute, TU Munich, 85748 Garching, Germany*

(Dated: February 2, 2008)

Abstract

We present spin relaxation times of 2D holes obtained by means of spin sensitive bleaching of the absorption of infrared radiation in p-type GaAs/AlGaAs quantum wells (QWs). It is shown that the saturation of inter-subband absorption of circularly polarized radiation is mainly controlled by the spin relaxation time of the holes. The saturation behavior has been determined for different QW widths and in a wide temperature range with the result that the saturation intensity substantially decreases with narrowing of the QWs. Spin relaxation times are derived from the measured saturation intensities by making use of calculated (linear) absorption coefficients for direct inter-subband transitions. It is shown that spin relaxation is due to the D'yakonov-Perel' mechanism governed by hole-hole scattering. The problem of selection rules is addressed.

PACS numbers: 72.25.Dc, 72.25.Rb

I. INTRODUCTION

The spin degree of freedom of charge carriers in semiconductors, being of fundamental interest as a dynamic variable, has recently attracted much attention in view of its possible role in active spintronic devices [1]. It is intimately related to the polarization degree-of-freedom of electromagnetic waves via the selection rules which have been used for optical spin orientation [2]. The spin relaxation times of electrons and holes in semiconductor quantum well structures have been measured for the first time in time-resolved photoluminescence experiments [3, 4, 5, 6]. In these investigations with optical excitations across the band gap, electron-hole pairs are created and the measured spin relaxation times reflect the particular situation of a bipolar spin orientation with relaxation processes, in which the electron-hole exchange process can play the dominant role [7]. This situation is not the one to be expected in prospective spintronic devices [8] which are likely to operate with one kind of carriers only, spin polarized electrons or holes, injected into the semiconductor via ferromagnetic contacts. For this situation the monopolar spin relaxation is the decisive dynamical quantity, whose dependence on device parameters needs to be investigated.

In spite of recent progress, the injection of spin polarized carriers through hetero-contacts remains a challenge and does not allow to measure spin relaxation times yet [9, 10]. Therefore, monopolar optical spin orientation combined with the photogalvanic effects (PGE), which has been demonstrated for n- and p-doped quantum well structures of different material compositions [11, 12], is the method of choice to investigate the spin dynamics of electrons or holes avoiding the problems connected with electrical spin injection. It has been demonstrated [13], that the linear and the circular PGE show a distinct saturation behavior with increasing intensity of the exciting light which carries information about the spin relaxation time. The analysis of these data requires the knowledge of the linear absorption coefficient for inter-subband transitions, which is difficult to measure and is hence provided by realistic calculations within the self-consistent multiband envelope function approximation [14].

We present here a detailed investigation of spin relaxation in rectangular p-type

(113)-grown GaAs/AlGaAs quantum wells of different widths L_W and in a wide temperature range. This first comprehensive experimental study of monopolar spin relaxation in dependence on these two relevant system parameters, width and temperature, is accompanied by a theoretical analysis that relates the measured spin relaxation times to the D'yakonov-Perel' mechanism.

The paper is organized as follows. First, we will present our samples and experimental technique and the results of the measurements. Following that, we outline the calculation of the absorption coefficient and by making use of this calculation derive the spin relaxation times. This is followed by a discussion of the dominant spin relaxation mechanism and the topic of selection rules.

II. EXPERIMENT

The experiments have been carried out on p-type (113) MBE-grown GaAs/AlGaAs QWs with widths L_W of 7, 10 and 15 nm. In order to improve sensitivity, multiple structures of 20 QWs were investigated. Samples with free carrier sheet densities p_s of about $2 \cdot 10^{11}$ cm^{-2} and a high mobility μ of around $5 \cdot 10^5\,\mathrm{cm}^2/(\mathrm{Vs})$ (at 4.2 K) were studied in the range from liquid helium temperature up to 140 K. At the samples a pair of Ohmic contacts is centered on opposite sample edges along the direction $x \,||\, [1\bar{1}0]$. As source of radiation a high power pulsed far-infrared (FIR) molecular laser, optically pumped by a TEA-CO_2 laser, has been used delivering 100 ns pulses with intensities up to 1 MW/cm^2 in the wavelength range between 76 μm and 148 μm providing direct inter-subband transitions from the lowest heavy hole $hh1$ to the light hole $lh1$ subband. The radiation of the FIR-laser is linearly polarized and a $\lambda/4$ plate was used to generate circularly polarized radiation with a polarization degree $P_{\mathrm{circ}} = \pm 1$ for right- and left-handed circularly polarized light.

The absorption of terahertz radiation by free carriers in QWs is weak due to their small thickness and difficult to measure in transmission experiments. This is even

worse in the case of bleaching at high power levels. Therefore, the nonlinear behavior of the absorption has been investigated employing the recently observed circular (CPGE) and linear (LPGE) photogalvanic effects [11, 12]. Both, CPGE and LPGE yield an easily measurable electrical current in x-direction. According to Ivchenko and Pikus [15] the nonlinear absorption coefficient is proportional to the photogalvanic current j_x normalized by the radiation intensity I. Thus, by choosing the degree of polarization, we obtain a photoresponse corresponding to the absorption coefficient of circularly or linearly polarized radiation.

The investigated intensity dependence of the absorption coefficient $\alpha \propto j_x/I$ shows saturation with higher intensities for all samples used in our experiments. It is observed that saturation takes place for excitation with circularly polarized radiation at a lower level of intensity compared to the excitation with linearly polarized radiation. The basic physics of this spin sensitive bleaching of absorption can be understood by looking at Fig. 1. Illuminating a p-type sample with FIR radiation of an appropriate wavelength results in direct transitions between the heavy-hole *hh1* and the light-hole *lh1* subbands. This process depopulates and populates selectively spin states in *hh1* and *lh1* subbands. The absorption is proportional to the difference of populations of the initial and final states. At high intensities the absorption decreases since the photoexcitation rate becomes comparable to the non-radiative relaxation rate back to the initial state. For C_s-symmetry, relevant for our (113)-grown QWs, the selection rules for the absorption at $\boldsymbol{k}$ close to zero are so that only one type of spin is involved in the absorption of circularly polarized light (a closer look at selection rules will be given at the end of this paper). Thus the absorption bleaching of circularly polarized radiation is governed by energy relaxation of photoexcited carriers and spin relaxation within the initial spin-split subband (see Figs. 1a and 1b). These processes are characterized by energy and spin relaxation times τ_e and τ_s, respectively. We note that during energy relaxation to the initial state in *hh1*, the holes loose their photoinduced spin orientation due to rapid relaxation [16]. Thus, spin orientation occurs in the initial subband *hh1*, only. In contrast to circularly polarized light, absorption of

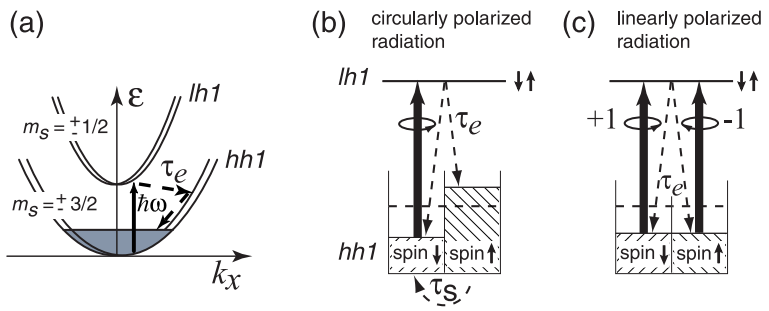

FIG. 1: Microscopic picture of spin sensitive bleaching: (a) direct *hh1-lh1* optical transitions, (b) and (c) process of bleaching for two polarizations. Dashed arrows indicate energy (τ_e) and spin (τ_s) relaxation.

linearly polarized light is not spin selective and the saturation is controlled by the energy relaxation only (see Fig. 1c). For $\tau_s > \tau_e$, bleaching of absorption becomes spin sensitive and the saturation intensity I_s of circularly polarized radiation drops below the value of linear polarization as indicated in Fig. 2 by arrows. The saturation intensity is defined as the intensity at which j_x/I is one half of its unsaturated value at $I \to 0$.

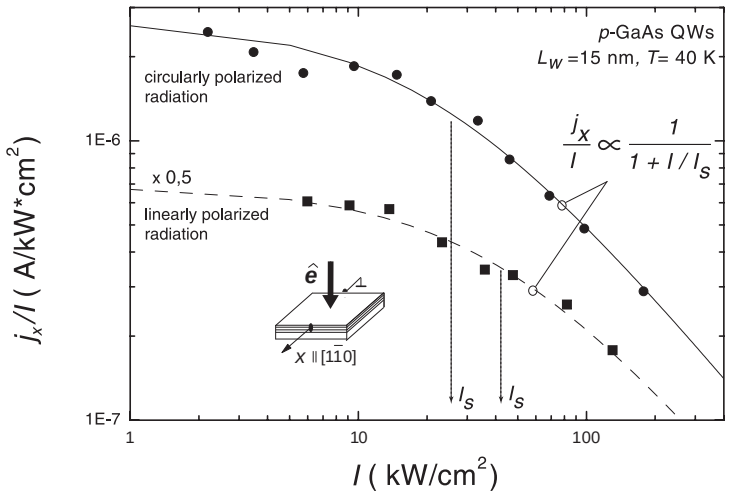

FIG. 2: CPGE and LPGE currents j_x normalized by the intensity as a function of the intensity for circularly and linearly polarized radiation of $\lambda = 148$ μm and at T = 40 K.

Fig. 3 presents the saturation intensities for different QW widths in the whole

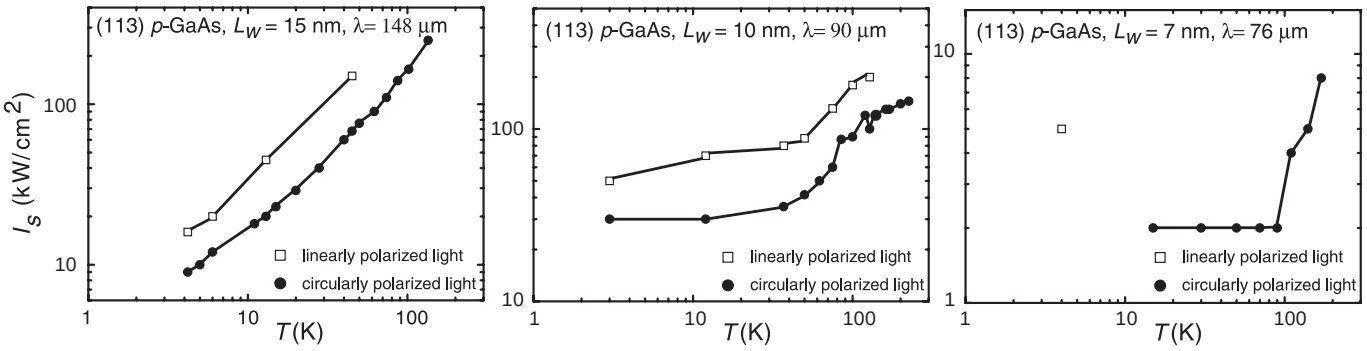

FIG. 3: Temperature dependence of the saturation intensities for various QW widths for linearly (open squares) and circularly (full circles) polarized light. The thickness of the QWs decreases from left to right.

investigated temperature range. Note that the saturation intensities I_s for the excitation with circularly polarized radiation (circles) are generally smaller than for linearly polarized radiation (squares). A significant reduction of the saturation intensities with decreasing L_W is observed and indicates longer hole spin relaxation times for narrower QWs, which has been shown theoretically in [16] for the first time.

The nonlinear behavior of the photogalvanic currents has been analyzed in terms of excitation-relaxation kinetics taking into account both optical excitation and non-radiative relaxation processes. It was shown [13] that the photocurrent j_{LPGE}, induced by linearly polarized radiation, is given by $j_{LPGE}/I \propto (1 + I/I_{se})^{-1}$, where I_{se} is the saturation intensity controlled by energy relaxation of the hole gas, while the photocurrent induced by circularly polarized radiation $j_{CPGE} \propto I/\left(1 + I\left({I_{se}}^{-1} + {I_{ss}}^{-1}\right)\right)$ in addition is controlled by spin relaxation with the term $I_{ss} = \hbar\omega p_s/(\alpha_0 L_W \tau_s)$. Here α_0 is the unsaturated absorption coefficient at low intensities. Thus the spin relaxation time τ_s is given by

$$\tau_s = \frac{\hbar\omega p_s}{\alpha_0 L_W I_{ss}} \tag{1}$$

III. ABSORPTION COEFFICIENT

In order to obtain τ_s with this formula from the measured saturation intensities I_{ss}, the value of α_0, not available from experiment, is determined theoretically. The calculations of the linear absorption coefficient α_0 for inter-subband transitions are based on the self-consistent multiband envelope function approximation (EFA) [14], that takes into account the crystallographic orientation of the QW (here the [113] direction) and the doping profile [1]. Calculations are performed within the Luttinger model of the heavy and light hole states to obtain the hole subband dispersion $\epsilon_i(\boldsymbol{k})$ and eigenstates $|i, \boldsymbol{k}\rangle$ of the hole subband i and in-plane wave-vector $\boldsymbol{k}$. For direct (electrical dipole) transitions between subbands i and j the contribution to the absorption coefficient $\alpha_{i\to j}(\omega)$ as a function of the excitation energy $\hbar\omega$ is then given by [17]

$$\alpha_{i\to j}(\omega) = \frac{e^2}{4\pi\epsilon_0\omega c n L_W} \int \mathrm{d}^2k \, |\langle j, \boldsymbol{k}|\boldsymbol{e}\cdot\hat{\boldsymbol{v}}(\boldsymbol{k})|i, \boldsymbol{k}\rangle|^2 \, [f_j(\boldsymbol{k}) - f_i(\boldsymbol{k})] \, \frac{\mathrm{e}^{-(\epsilon_j(\boldsymbol{k})-\epsilon_i(\boldsymbol{k})-\hbar\omega)^2/\Gamma^2}}{\sqrt{\pi}\Gamma} \,, \tag{2}$$

where $\boldsymbol{e}$ is the light polarization vector, n is the refractive index, ϵ_0 is the free-space permittivity, $f_i(\boldsymbol{k})$ is the Fermi distribution function in the subband i and Γ is a phenomenological parameter to account for the level broadening due to scattering. Within EFA, the velocity $\hat{\boldsymbol{v}}(\boldsymbol{k})$ is a matrix operator expressed as the gradient in $\boldsymbol{k}$-space of the Luttinger Hamiltonian. Its matrix elements are calculated from the EFA wave functions.

Following this scheme we calculate the absorption coefficient $\alpha_0(\omega) = \sum_{ij} \alpha_{i\to j}(\omega)$. The absorption spectrum for the system with $L_W = 7\,\mathrm{nm}$ is shown in Fig. 4a. At low temperatures two pronounced peaks evolve, which correspond to the transitions from the lowest (spin split) hole subband to the second and third subband, respectively. Fig. 4b shows the temperature dependence (due to the Fermi distribution function)

[1] In accordance with the growth parameters of the samples, we assumed an acceptor concentration of $1\cdot10^{16}\,\mathrm{cm}^{-3}$ in the barriers and a spacer width of 70 Å (45 Å) on the left (right) side of the well. The values of the band parameters are identical with those given in: L. Wissinger, U. Rössler, B. Jusserand, and D. Richards, Phys. Rev. B **58**, 15375 (1998).

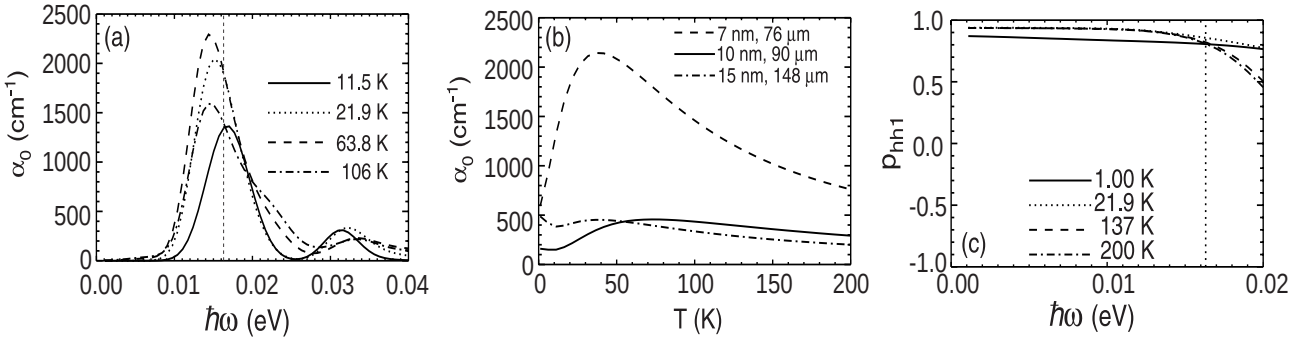

FIG. 4: (a) Calculated absorption coefficient α_0 for a QW with L_W= 7 nm as a function of photon energy $\hbar\omega$ for various temperatures T and (b) as a function of T for various QW widths with $\hbar\omega$ corresponding to the energy of the exciting laser light. (c) Hole spin orientation efficiency p_{hh1} (see chapter *selection rules and spin orientation*) as a function of $\hbar\omega$ for different T, L_W= 7 nm and right handed circular polarization. All calculations were performed for a carrier density p_s of about $2 \cdot 10^{11}\,\mathrm{cm}^{-2}$ and a broadening $\Gamma = 2.47\,\mathrm{meV}$.

of α_0 at the respective excitation energies for the different samples. The calculated values of α_0 are used to convert the measured saturation intensities I_{ss} according to Eq. (1) into spin relaxation times τ_s.

The resulting hole spin relaxation times in dependence on the temperature are shown in Fig. 5 for QWs of different widths. Our measurements show longer hole spin relaxation times for narrower QWs. Note the different behavior of the spin relaxation times with the temperature for different QW widths. It is worth mentioning that at high temperatures a doubling of the QW width decreases τ_s by almost two orders of magnitude. Compared to the values given in [13] (for L_W = 15 nm), where α_0 was derived from [17], we obtain here smaller τ_s at higher temperatures due to a more realistic theoretical model for the calculation of α_0.

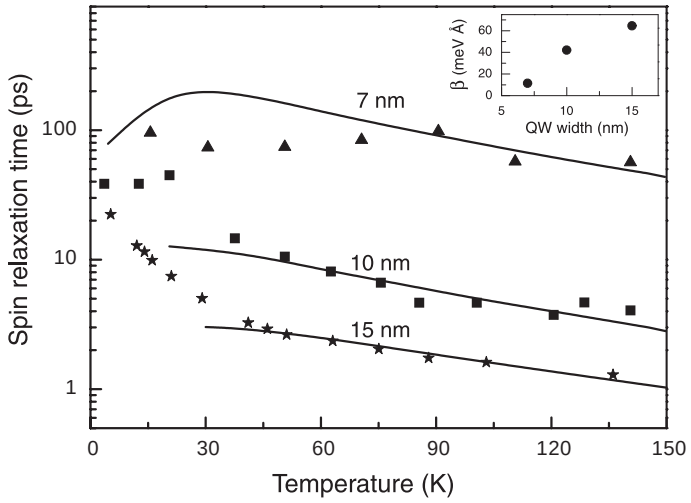

FIG. 5: Spin relaxation times of holes for three different widths of (113)-grown GaAs/AlGaAs QWs as a function of temperature. The solid lines show a fit according to the D'yakonov-Perel' relaxation mechanism. The inset shows the hole spin-splitting parameter β obtained from the fit.

TABLE I: Momentum relaxation times τ_p (determined from mobility) and the ratios τ_p/τ_s for different QW widths at 4.2 K.

QW width (nm)	τ_p (ps)	τ_p/τ_s
7	9.5	0.1
10	25	0.64
15	38	1.73

IV. SPIN RELAXATION MECHANISM

In order to understand the mechanism governing spin relaxation, we consider the ratio of momentum τ_p and spin τ_s relaxation times at $T = 4.2$ K presented in Table I. In the p-doped QWs, studied here, there are two possible routes to hole spin relaxation: the Elliot-Yafet and the D'yakonov-Perel' mechanism. In the first case, spin is lost during scattering. However the ratio τ_p/τ_s for holes, where τ_p is determined from mobility measurements, has a strong dependence on the QW width ($\sim L_W^6$) for

scattering from impurity or interface micro-roughness. Note that for the calculation of the spin relaxation time we do not take into account phonon scattering because most of the experimental data belongs to the range of low temperatures where phonon scattering processes play an unimportant role. In addition, τ_p is of the same order as τ_s for the two wider QWs which contradicts the main idea of the Elliot-Yafet mechanism. Another possibility is the Elliot-Yafet spin relaxation controlled by hole-hole collisions, but for this mechanism asymmetry of the QW heteropotential is needed [18].

We conclude that the Elliot-Yafet mechanism is unimportant in the structures under study, since the experiment shows a too weak dependence for τ_p/τ_s on the QW width. The above experimental results suggest much longer spin relaxation times for the given mobilities than expected for the Elliot-Yafet mechanism. The spin relaxation time at helium temperature according to Elliot-Yafet mechanism can be estimated as

$$\tau_s \approx \tau_p \left(\frac{k_{\rm F} L_W}{\pi} \right)^{-6}$$

where $\boldsymbol{k}_{\rm F}$ is the Fermi wave-vector. This yields $\tau_s \approx 5 \times 10^5$ ps which is three orders of magnitude larger than measured values. Therefore, the main mechanism of hole spin relaxation is the D'yakonov-Perel' one [19]: hole spin is lost between the scattering events. For this mechanism, the spin relaxation rate is given by the expression

$$\frac{1}{\tau_s} = \left(\frac{\beta}{\hbar} \right)^2 k_{\rm F}^2 \, \tau^*, \tag{3}$$

where β is the spin-splitting coefficient of the $\boldsymbol{k}$-linear terms in the Hamiltonian yielding

$$E_{3/2}(k) - E_{-3/2}(k) = 2 \, \beta \, k.$$

The time τ^* is the microscopic scattering time which has contributions from both momentum scattering and carrier-carrier collisions [20]. We have calculated the hole-hole scattering time governing the D'yakonov-Perel' spin relaxation mechanism by solving the quantum kinetic equation for the hole pseudospin density matrix similar to Ref. [21]. Our calculation shows that the hole-hole scattering time is shorter than τ_p at 4.2 K. We believe that in the relevant temperature range τ_p does not change

significantly. Therefore, hole-hole scattering controls D'yakonov-Perel' spin relaxation in the whole temperature range.

Fig. 5 presents spin relaxation times extracted from the experiment (points) together with a theoretical fit using Eq. (3) (solid lines) showing a good agreement between theory and experiment. The discrepancy at low lattice temperatures may be attributed to the fact that the hole gas is not in equilibrium due to optical pumping. This case requires special theoretical treatment.

In the inset the hole spin-splitting parameter β obtained from the fit is plotted as a function of the QW width. The corresponding spin splitting is equal to 0.17, 0.68, and 1.32 meV for QW widths 7, 10, and 15 nm, respectively. This order of magnitude agrees with hole spin-splitting obtained from multiband calculations [22]. The parameter β increases with the QW width. This is a specific feature of 2D hole systems where spin-splitting is determined by heavy-light hole mixing which is stronger in wider QWs [23].

V. SELECTION RULES AND SPIN ORIENTATION

For the definition of I_{ss} we assumed that the spin selection rules are fully satisfied at the transition energy. This is the case for optical transitions occurring close to $\boldsymbol{k} = 0$ in (001)-grown systems [24]. However, in (113)-grown systems, heavy-hole and light-hole subbands are strongly mixed, even at $\boldsymbol{k} = 0$. This reduces the strength of the selection rules and therefore the efficiency of spin orientation. The mixing can be taken into account by means of a multiplicative factor in I_{ss}, which increases the saturation intensity at constant spin relaxation time [25].

The lowest subband, which for (001)-grown systems is purely heavy hole ($m_s = \pm 3/2$) at $\boldsymbol{k} = 0$, has for growth direction [113] an admixture of about 10% light hole spinor components ($m_s = \pm 1/2$) [26]. This admixture is sufficiently small to justify subband labeling according to the dominant spinor component at $\boldsymbol{k} = 0$.

Strict selection rules for inter-subband transitions between hole subbands only exist

for some idealized limits (e.g. spherical approximation for the Luttinger Hamiltonian or growth directions of high symmetry and $\boldsymbol{k} = 0$). However, assuming a symmetrically doped (113)-grown QW, the lowest *hh* and *lh* subband states (*hh1* and *lh1*, respectively) have even parity at $\boldsymbol{k} = 0$ and no transition between *hh1* and *lh1* is possible, as the velocity operator projected on the light polarization direction $\hat{\boldsymbol{v}} \cdot \boldsymbol{e}$ couples only states of different parity. Therefore a strictly valid selection rule cannot be obtained and a more quantitative discussion of the relative weight of the possible transitions is necessary. For $\boldsymbol{k}$ small enough to ensure that the admixture of odd parity spinor components is negligible, only contributions in $\hat{\boldsymbol{v}} \cdot \boldsymbol{e}$ linear in $\boldsymbol{k}$ are to be considered.

A more detailed analysis gives the following results: The spin-conserving transitions $hh1 \uparrow \rightarrow lh1 \uparrow$ and $hh1 \downarrow \rightarrow lh1 \downarrow$ are much weaker than the corresponding spin-flip transitions $hh1 \uparrow \rightarrow lh1 \downarrow$ and $hh1 \downarrow \rightarrow lh1 \uparrow$. Depending on the left/right circular polarization of the exciting light, one of the spin-flip transitions is dominant. To investigate the hole spin orientation, we also performed a numerical calculation of $\alpha_{i \rightarrow j}$ for excitation with right-hand circularly polarized light. We obtained that the transition $hh1 \downarrow \rightarrow lh1 \uparrow$ is far more probable than all other transitions. This is quantitatively described by the heavy hole spin polarization efficiency

$$p_{hh1} = \frac{\sum_i \alpha_{hh1\downarrow \rightarrow i} - \alpha_{hh1\uparrow \rightarrow i}}{\sum_i \alpha_{hh1\downarrow \rightarrow i} + \alpha_{hh1\uparrow \rightarrow i}} \,, \tag{4}$$

where the summation is performed over all subbands. If p_{hh1} is $+1$ (-1) the excitation leaves only heavy holes belonging to the up (down) branch of the dispersion in the *hh1* subband. In our case, p_{hh1} is around 80 % at the laser excitation energy and almost independent of the temperature (Fig. 4c). Therefore we may neglect effects due to incomplete spin orientation, as assumed in this contribution.

In conclusion our experimental results demonstrate a strong dependence of the hole spin relaxation times on the width of the quantum well. With wider QWs, the spin relaxation times become much shorter. At high temperatures, a doubling of the QW width results in a changing of the magnitude in two orders. Theoretical calculations in comparison to quantitative experimental results show that the D'yakonov-Perel'

mechanism controlled by hole-hole collisions dominates the spin relaxation process.

The authors thank E. L. Ivchenko for helpful discussions and fruitful comments. Financial support from the DFG, the RFBR, "Dynasty" Foundation — ICFPM and INTAS is gratefully acknowledged.

[1] D. D. Awschalom, D. Loss, and N. Samarth, Semiconductor spintronics and quantum computation, in *Nanoscience and technology*, edited by K. von Klitzing, H. Sakaki, and R. Wiesendanger, Springer, Berlin, 2002.

[2] G. E. Pikus and A. N. Titkov, Spin relaxation under optical orientation in semiconductors, in *Optical Orientation*, edited by F. Meier and B. P. Zakharchenya, Elsevier, Amsterdam, 1984.

[3] T. C. Damen, L. Viña, J. E. Cunningham, J. Shah, and L. J. Sham, Phys. Rev. Lett. **67**, 3422 (1991).

[4] M. Kohl, M. R. Freeman, D. D. Awschalom, and J. M. Hong, Phys. Rev. B **44**, 5923 (1991).

[5] A. Tackeuchi, Y. Nishikawa, and O. Wada, Appl. Phys. Lett. **68**, 797 (1996).

[6] R. Terauchi et al., Jpn. J. Appl. Phys. **38**, 2549 (1999).

[7] G. L. Bir, A. G. Aronov, and G. E. Pikus, Zh. Eksp. Teor. Fiz. **69**, 1382 (1975), [Sov. Phys. JETP **42**, 705 (1976)].

[8] S. Datta and B. Das, Appl. Phys. Lett. **56**, 665 (1990).

[9] Y. Ohno et al., Nature **402**, 790 (1999).

[10] G. Schmidt, D. Ferrand, L. W. Molenkamp, A. T. Filip, and B. J. van Wees, Phys. Rev. B **62**, R4790 (2000).

[11] S.D. Ganichev, E.L. Ivchenko, H. Ketterl, W. Prettl, and L.E. Vorobjev, Appl. Phys. Lett. **77**, 3146 (2000).

[12] S.D. Ganichev, E. L. Ivchenko, S.N. Danilov, J. Eroms, W. Wegscheider, D. Weiss, and W. Prettl, Phys. Rev. Lett. **86**, 4358 (2001).

[13] S.D. Ganichev, S.N. Danilov, V.V. Bel'kov, E.L. Ivchenko, M. Bichler, W. Wegscheider, D. Weiss, and W. Prettl, Phys. Rev. Lett. **88**, 057401 (2002).

[14] R. Winkler and U. Rössler, Phys. Rev. B **48**, 8918 (1993).

[15] E.L. Ivchenko and G.E. Pikus, *Superlattices and Other Heterostructures. Symmetry and Optical Phenomena*, (Springer, Berlin 1997).

[16] R. Ferreira and G. Bastard, Phys. Rev. B. **43**, 9687 (1991).

[17] L.E. Vorobjev, D.V. Donetskii, and L.E. Golub, Pis'ma ZhETF **63**, 977 (1996) [JETP Lett. **63**, 981 (1996)]

[18] M.M. Glazov and E.L. Ivchenko, unpublished.

[19] G. Bastard and R. Ferreira, Europh. Lett. **23**, 439 (1993).

[20] M.M. Glazov and E.L. Ivchenko, Pis'ma ZhETF **75**, 476 (2002) [JETP Lett. **75**, 403 (2002)].

[21] M.M. Glazov, E.L. Ivchenko, M.A. Brand, O.Z. Karimov, and R.T. Harley, Proc. 11th Int. Symp. "Nanostructures: Physics and Technology", St.Petersburg, 2003, p. 273; cond-mat/0305260.

[22] R. Winkler, Phys. Rev. B. **62**, 4245 (2000).

[23] R. Winkler, H. Noh, E. Tutuc, and M. Shayegan, Phys. Rev. B **65**, 155303 (2002).

[24] S. Jorda and U. Rössler, Superlatt. Microstruct. **8**, 481 (1990).

[25] S.D. Ganichev, V.V. Bel'kov, S.N. Danilov, E.L. Ivchenko, H. Ketterl, L.E. Vorobjev, M. Bichler, W. Wegscheider, and W. Prettl, Physica E **10**, 52 (2001).

[26] R. Winkler and A. I. Nesvizhskii, Phys. Rev. B. **53** , 9984 (1996).